Article No. jmbi.1999.3126 available online at http://www.idealibrary.com on IDEAL® J. Mol. Biol. (1999) 293, 639–651

JMB

Detergents Modulate Dimerization, but not Helicity, of the Glycophorin A Transmembrane Domain

Lillian E. Fisher[1,2], Donald M. Engelman[2,3]* and James N. Sturgis[4]

[1]*Department of Chemistry*

[2]*Department of Molecular Biophysics and Biochemistry Yale University, New Haven CT, USA*

[3]*Professeur de Recherche Blaise Pascal, Region Ile de France France*

[4]*Laboratoire d'Ingenierie des Systemes Macromoléculaires Institut de Biologie Structurale et Microbiologie, CNRS Marseilles, France*

**Corresponding author*

Understanding how the lipid environment influences transmembrane helix association requires thermodynamic measurements that can be interpreted in terms of specific chemical interactions. We have used Förster resonance energy transfer to measure dimerization of the glycophorin A transmembrane helix in detergent micelles. The observed K_d is at least two orders of magnitude weaker in sodium dodecyl sulfate than it is in zwitterionic detergents. In contrast, neither dimerization nor the detergent affects the secondary structure of the glycophorin A helix as measured by far-UV circular dichroism. These measurements support a long standing assumption about the glycophorin A transmembrane domain, that detergents uncouple helix formation from helix dimerization. The approach is applicable to a variety of systems in diverse environments, extending our ability to measure how interactions with complex solvents affect the thermodynamics of oligomerization.

Keywords: thermodynamics; integral membrane protein; protein-lipid interactions; fluorescence; FRET

Introduction

Understanding how features of the lipid environment such as thickness, fluidity, and composition influence the folding and oligomerization of membrane proteins has been limited by a lack of thermodynamic data (Haltia & Friere, 1995; Killian, 1998; Lee, 1998; Mouritsen & Bloom, 1993; Stowell & Rees, 1995; van Klompenburg *et al*., 1997). The insolubility of membrane-spanning helices in aqueous solutions complicates investigation of their folding and assembly (Popot & de Vitry, 1990; White & Wimley, 1998), even though their hydrophobic nature facilitates their identification in sequenced genomes (Boyd *et al*., 1998; Wallin & von Heijne, 1998). New approaches, such as the one presented here, are being developed to identify reversible steps in membrane protein folding pathways and to measure how they are thermodynamically coupled to environmental properties (Booth *et al*., 1997; Huang *et al*., 1981; Lau & Bowie, 1997; Sturgis & Robert, 1994). Popot & Engelman (1990) hypothesized that the formation of individual transmembrane helices may be energetically distinct from their assembly into helical bundles and oligomeric structures. They proposed that stable helical domains are formed in stage I through hydrogen bonding and insertion into a membrane, which subsequently assemble in stage II to form tertiary and quaternary structures.

Dimerization of the human erythrocyte protein glycophorin A has proven to be an instructive example of a stage II reaction. The glycophorin A transmembrane domain (GpA) lacks bound pigments or cofactors, forms stable helical dimers in the absence of the soluble domains, and can be reversibly assembled in a variety of environments. The structure of the dimer has been solved by NMR in dodecyl phosphocholine micelles (DPC) (MacKenzie *et al*., 1997) and the association of GpA has been investigated in pure phospholipid bilayers (Adair & Engelman, 1994; Sami & Dempsey, 1988; Smith *et al*., 1994), in the *Escherichia coli* inner membrane (Langosch *et al*., 1996; Leeds & Beckwith, 1998; Russ & Engelman, 1999), and computationally (Adams *et al*., 1996; Treutlein *et al*., 1992).

Abbreviations used: CD, far-UV circular dichroism; CMC, critical micelle concentration; Cou, 7-dimethylaminocoumarin-4-acetayl Cou·GpA, GpA labeled with Cou at the N terminus; DDMAB, dodecyl-*N*,*N*-dimethyl ammonium butyrate; DPC, dodecyl phosphocpholine; FRET, Förster resonance energy transfer; GpA, human glycophorin A residues 69-101; Pyr, 1-pyrene acetyl; Pyr·GpA, GpA labeled with Pyr at the N terminus; SN/GpA, Staphylococcal nuclease-GpA chimera.

E-mail address of the corresponding author: don@paradigm.csb.yale.edu

0022-2836/99/430639–13 $30.00/0

All the thermodynamic experiments so far reported have used a chimeric protein developed by Lemmon *et al*. (1992a) in which the transmembrane domain of GpA is attached to the nuclease from *Staphylococcus aureus* (SN/GpA). Using the SN/GpA chimera allows the expression of many mutants that can be purified from *E. coli* and facilitates assessment of dimerization from changes in the apparent molecular mass. The relative amount of dimer in SDS-PAGE was used to assess the effect of single mutations on dimerization (Lemmon *et al*., 1992b). The assay has since been extended to include single and multiple insertions (Mingarro *et al*., 1997).

Recently, measurements of the SN/GpA dimer structure and its sensitivity to mutation have been extended to less denaturing detergent environments. The SN/GpA parallel dimer has been measured in a zwitterionic detergent, *N*-dodecyl-*N*,*N*-dimethyl-4-amino butyrate (DDMAB) using small-angle X-ray scattering (Bu & Engelman, 1999). The stability of the wild-type dimer precluded measurement of the equilibrium constant, but the effect of a destabilizing mutation was measurable by this new method. Dissociation constants of SN/GpA and single-point mutants have been measured in the non-ionic detergent polyoxyethylene-5-octyl ether using analytical ultracentrifugation (Fleming *et al*., 1997). These measurements provide the first relative scale of the sequence-dependent stability of the GpA dimer, although the precise chemical and thermodynamic interpretation of the data remains at an early stage (MacKenzie & Engelman, 1998). While each of these approaches has unique advantages, each technique is also dependent on specific micelle properties: on negative charge in SDS-PAGE, on matching the electron density in small-angle X-ray scattering, and on matching the buoyant density in analytical ultracentrifugation.

A complete investigation of GpA dimerization must ultimately include the coupled equilibria involving the detergent illustrated in Figure 1(a): detergent binding to the peptide monomer, detergent binding to the peptide dimer, and micelle formation. Each state available to the detergent involves a different number of detergent molecules (x, y, or z) associating with a distribution of binding constants. Furthermore, the detergent activity is not a simple function of concentration as the activity coefficient changes dramatically at the critical micelle concentration (CMC), becoming much less than unity. The detectable molecular species illustrated in Figure 1(b), i.e. the monomeric and dimeric peptides with their respective detergent environments, reflect the relative partitioning of the dissolved monomeric detergent between the three complexes. Thus, the observed equilibrium includes environmental terms as shown in equation (1):

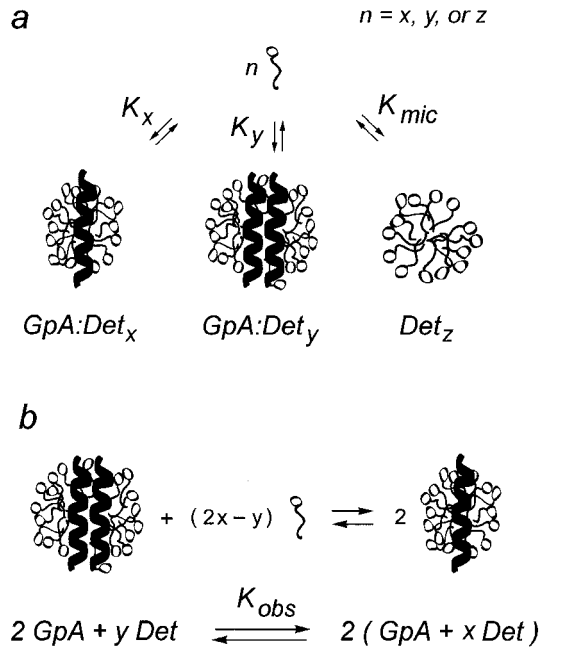

Figure 1. Observed GpA dissociation. (a) A detergent molecule may remain dissolved as a monomer (top), bind to the surface of monomeric GpA (bottom left), bind to the surface of dimeric GpA (bottom middle), or self-associate to form micelles (bottom right). (b) The coupled equilibria involving the detergent are detected indirectly through their effect on GpA dissociation. The two measurable species in this study are the dissolved GpA dimer with an average of *y*-bound detergent molecules (left), and the dissolved GpA monomer with an average of *x*-bound detergent molecules (right).

$$K_{\text{observed}} = K_{\text{GpA}} \frac{K_x^2}{K_y K_{\text{mic}}} \qquad (1)$$

where K_x and K_y are the equilibrium constants describing detergent binding to the monomer and dimer peptides, and K_{mic} is the equilibirum constant reflecting detergent self-association. The environmental term will only be small when the fraction K_x^2/K_yK_{mic} is close to unity. As a first step toward understanding transmembrane helix association in specific chemical and thermodynamic terms we sought to determine if the effect of the environment on helix association was large enough to be measured and if it could be separated from the effect of the environment on helix formation.

Förster resonance energy transfer (FRET) has been widely used to measure relative distances in proteins and nucleic acids (van der Meer *et al*., 1994; Stryer, 1978), but less frequently to measure kinetic and thermodynamic properties of oligomeric complexes (Patel *et al*., 1994; Veatch & Stryer, 1977; Wendt *et al*., 1995). The possibility of very low dissociation constants for membrane helix oligomerization and the high sensitivity of fluorescence make FRET a useful technique for this type of study. We have used peptides labeled

uniquely and completely with small fluorescent probes to measure the dissociation constant of the GpA dimer and its sensitivity to the environment. Combined with far-UV circular dichroism (CD) spectroscopy to measure the average secondary structure of the monomeric and dimeric GpA, we demonstrate the utility of the approach in anionic and zwitterionic detergent micelles.

Results and Discussion

Experimental design

Measuring how the environment affects the thermodynamics of GpA dimerization requires a sensitive indicator of GpA monomer and dimer concentrations that can be applied in both micelles and lipid bilayers. The primary sequence of the transmembrane domain of human glycophorin A, including the hydrophobic region and flanking amino acids expected to interact with the polar head groups of the lipids, is shown in Figure 2(a).

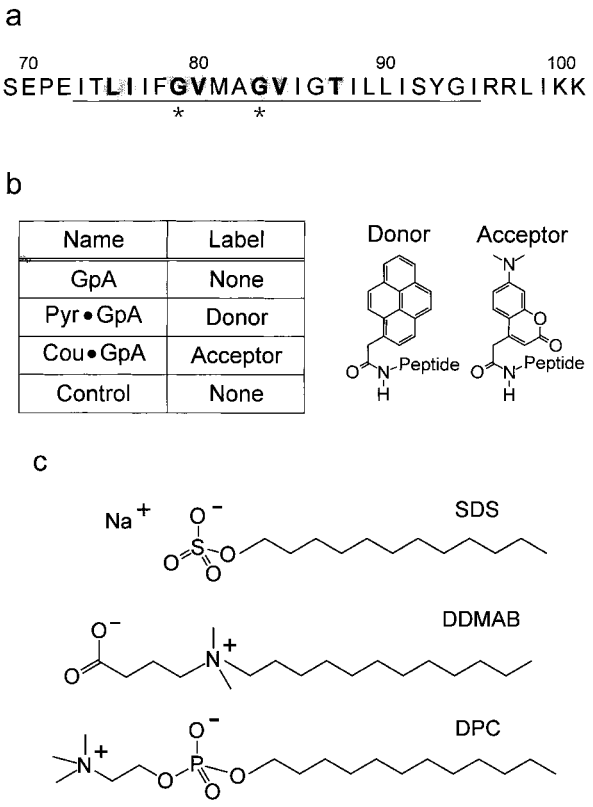

Figure 2. Glossary of molecules. (a) The sequence of the human GpA transmembrane domain showing the hydrophobic region (underlined) and residues at the dimer interface (boxed in gray). The labels were attached to the N terminus on the left. A monomeric control peptide has leucines in place of the two glycines marked by asterisks below their positions. (b) GpA designates the unlabeled wild-type sequence, Pyr·GpA and Cou·GpA designate the pyrene donor and the coumarin acceptor at the N terminus, and Control designates the unlabeled double mutant. The structures of the labels conjugated to the N terminus. (c) The detergents used in this study, SDS, DDMAB, and DPC.

To use Förster resonance energy transfer as a measure of peptide association, pyrene (Pyr) and 7-dimethylaminocoumarin (Cou) were selected as a donor-acceptor pair (Haugland, 1996). A synthetic approach allowed the fluorescent labels to be attached uniquely and completely through condensation of a carboxylic acid derivative with the amino terminus of the polypeptide. As displayed in Figure 2(b) we will refer to the peptides using a prefix that refers to the identity of the label. An unlabeled monomeric control peptide was synthesized with leucine residues in place of glycine residues at positions 79 and 83. Each Gly to Leu mutation abolished dimerization in SDS-PAGE (Lemmon *et al.*, 1992b).

The three dodecyl detergents examined in this study (Figure 2(c)) allow us to test the utility of our approach by drawing on what is known about the GpA dimer from other methods. SDS was used to explore the unusual stability of the wild-type GpA dimer and to establish a thermodynamic foundation for the extensive mutagenesis in SDS-PAGE (Lemmon *et al.*, 1992b). DDMAB and DPC are zwitterionic detergents thought to be more native-like than SDS. Independent structural data showing a parallel helix dimer are available in all three detergents (Bu & Engelman, 1999; Lemmon *et al.*, 1992b; MacKenzie *et al.*, 1997).

Characterization of labeled peptides

The effect of labeling was assessed to ensure that the attached fluorophores provided a sensitive measure of concentration without significantly altering the secondary structure of the peptide. The experimentally determined molar absorptivity of the labeled peptides at their absorption maxima are 32,000(±2600) l mol^{-1} cm^{-1} at 344 nm for Pyr·GpA and 16,500(±3200) l mol^{-1} cm^{-1} at 378 nm for Cou·GpA. Relative to the free dyes in methanol (Haugland, 1996) the absorption maxima were red-shifted <10 nm and the extinction coefficients of the fluorophores attached to the peptide were reduced by 20 % to 25 % after reconstitution into detergent micelles. Since both chromophore conjugation and interactions with the local environment may have large effects on the absorbance and quantum yield, the small red-shift and moderate reduction is not surprising.

Far-UV circular dichroism spectroscopy was used to detect whether fluorescent labeling affected the secondary structure of the GpA peptide. The CD spectra shown in Figure 3 all have a maximum near 194 nm and double minima near 208 nm and 222 nm, which are characteristic of α-helical secondary structure. The spectra of the labeled and unlabeled GpA peptides were indistinguishable in the three detergents, showing that the strong UV absorbance of the fluorophores does not affect the measured spectra. Furthermore, the spectra of the dimeric GpA peptides are identical to the spectra of monomeric control peptides. The spectrum of monomeric GpA, which is measurable only in SDS

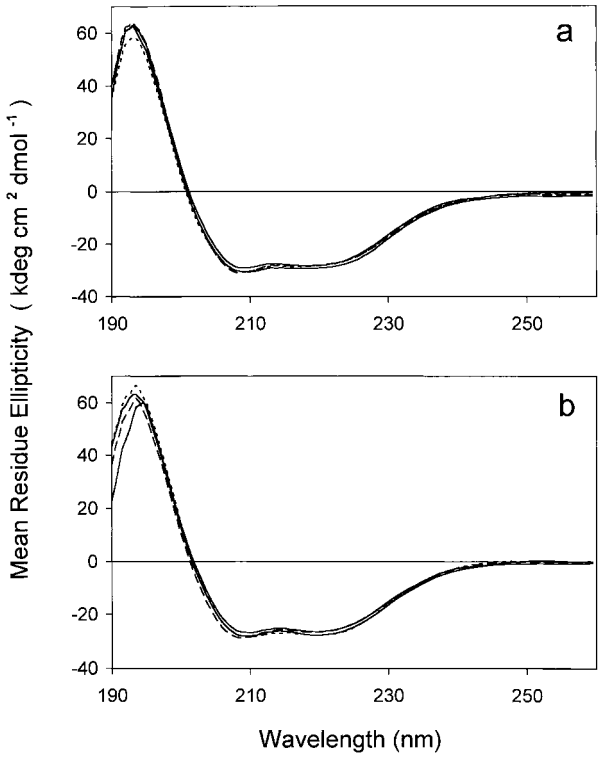

Figure 3. Secondary structure of the peptides. Far-UV circular dichroism spectra of each peptide was collected in each detergent; unlabeled GpA (- - -), Pyr·GpA and Cou·GpA (—), unlabeled control (– – –); (a) 25 mM SDS; (b) 25 mM DPC. Spectra obtained at other detergent concentrations and in DDMAB were the same as the spectra shown. The measured ellipticity was converted to mean residue ellipticity (MRE) as described in Materials and Methods.

because of the dimer stability, is also the same (data not shown). The mean residue ellipticity is 60(±3) kdeg cm^2 dmol^{-1} at 194 nm, −28(±2) kdeg cm^2 dmol^{-1} at 208 nm, and −28(±1) kdeg cm^2 dmol^{-1} at 222 nm. These values are independent of peptide and detergent concentration and are consistent with largely α-helical polypeptides, which neither change secondary structure nor are subject to super-helical twisting upon association (Zhou *et al.*, 1992). CD measurements of GpA peptides in other environments (Schulte & Marchesi, 1979; Smith *et al.*, 1994) are similar to the helicity we have measured, which includes the detergent (DPC) in which the NMR structure of the GpA dimer was solved (Figure 3(b)) (MacKenzie *et al.*, 1997). This result confirms that GpA helix formation is uncoupled from dimerization, in stark contrast to the coupling between the random coil monomer and helical oligomer observed in soluble helix assocation reactions. Together, the UV and CD data show that we can reproducibly assemble the labeled GpA peptides in SDS, DDMAB, and DPC micelles, and justify our confidence in comparing thermodynamic measurements between them.

The SN/GpA chimera was used in the SDS-PAGE assay to determine whether fluorescent labeling interfered with formation of chimera-peptide heterodimers (Lemmon *et al.*, 1992b). An experiment comparing the migration of the SN/GpA chimera in the presence of labeled and unlabeled peptides is shown in Figure 4. The first lane shows two bands corresponding to chimera monomer and dimer. Addition of peptides in lanes 2-4 results in the appearance of a band that migrates between the monomer and dimer bands. This third band corresponds to the expected migration of the chimera-peptide heterodimer, demonstrating that the labeled peptides compete for the helix-helix binding sites. The bands in lane 2, in which unlabeled peptide was added, are the same as the bands in lanes 3 and 4, in which labeled peptides were added, showing that the labels have no measurable effect on the ability of the peptides to compete with the SN/GpA chimera. The control in lane 5 does not exhibit a heterodimer band confirming that this application of the SDS-PAGE assay retains the expected sequence specificity. Formation of chimera-peptide heterodimer demonstrates that although the dimers are unusually stable, the transmembrane helices comprising the GpA dimer are able to exchange with one another.

Evidence of sequence-dependent Förster resonance energy transfer

The donor and acceptor fluorophores were chosen to provide a FRET signal that is insensitive to the details of the dimer structure but sensitive to the amount of dimer present. The excitation and emission spectra of the labeled peptides shown in Figure 5 display advantageous properties of the fluorophores. The donor (Figure 5(a)) has a high extinction coefficient and there is good overlap of its emission spectrum with the acceptor absorption spectra (Figure 5(b)). Furthermore, pyrene has a high quantum yield and narrow bands allowing for easy detection of energy transfer through sensitized acceptor emission. Measurement of the donor fluorescence yield gave a value of 25% for

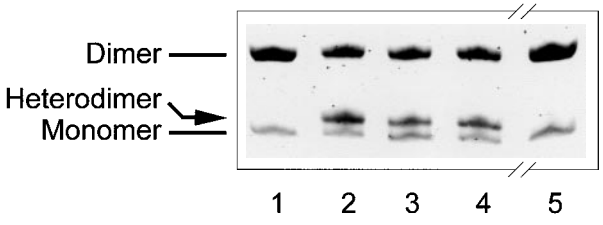

Figure 4. SDS-PAGE competition assay. All the samples have 15 μM SN/GpA chimera (Lemmon *et al.*, 1992a) with various peptides added at a chimera:peptide ratio of 2:1 (mol:mol). Added peptide: lane 1, none; lane 2, unlabeled GpA; lane 3, Pyr·GpA; lane 4, Cou·GpA; lane 5, control peptide (a non-dimerizing double mutant, GpA G79L, G83L).

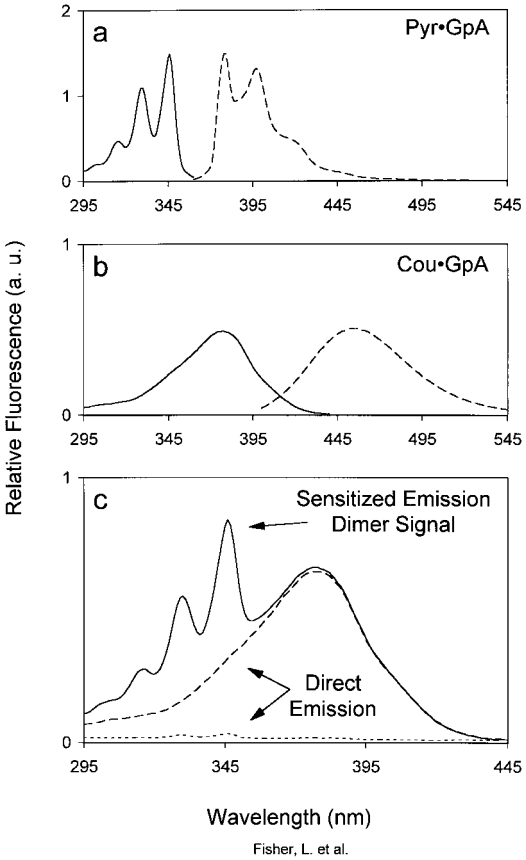

Figure 5. Fluorescence spectra of labeled GpA peptides. Excitation spectra (—) and emission spectra (– – –) were collected at peptide concentrations of 2.0 μM. (a) Pyr·GpA, excitation $\lambda = 345$ nm, emission $\lambda = 378$ nm. (b) Cou·GpA, excitation $\lambda = 378$ nm, emission $\lambda = 460$ nm. Except for the excitation and emission λ the instrument parameters were the same for (a) and (b). (c) The emission intensity was measured at 500 nm as a function of excitation wavelength for an equimolar mixture of donor and acceptor peptides at a total peptide concentration of 4.0 μM (—) and for separate samples of donor (---) and acceptor (– – –) peptides at 2.0 μM. The spectra were measured in buffered solutions containing 25 mM DDMAB and are similar to spectra obtained in SDS and DPC (data not shown).

Pyr·GpA in SDS, well within the expected range for pyrene (van der Meer *et al.*, 1994). Together with the measured quantum yield, spectra similar to those shown in Figure 5 were used to calculate the overlap integral for this donor-acceptor pair, and thus to calculate the Förster radius (R_0), the distance at which the probability of the energy transfer through a Förster mechanism is 50% (Stryer, 1978). R_0 for FRET between Pyr·GpA and Cou·GpA is 60(±5) Å. Assuming random fluorophore orientations, this pair might be used for distance measurements in the range of 40-90 Å because FRET depends on the inter-fluorophore separation to the inverse sixth power. According to the NMR data, backbone atom mobility near the amino terminus is much higher than in the helical region (MacKenzie, 1997), which should allow for rapid reorientation of the labels. The distance between amino termini in the GpA dimer was estimated to be in the range of 10-20 Å (MacKenzie *et al.*, 1997). Therefore, because the labels are likely to have variable orientations and the distance between donor and acceptor is expected to be considerably less than R_0, FRET was not likely to be limited by the distance between or relative geometry of the fluorophores.

An alternative to measuring FRET by donor emission quenching is sensitized acceptor emission, which may be used to detect FRET even when interactions with the environment may affect the donor quantum yield differently in the monomer and dimer states. In this approach, energy transfer is detected by scanning the excitation wavelength while observing the emission at a fixed wavelength. As shown in Figure 5(c), the excitation spectra of donor and acceptor labeled peptides were measured separately and compared to the excitation spectrum after they were mixed. The emission detected at 500 nm is plotted as a function of excitation wavelength from 295 to 445 nm. At 500 nm the fraction of the emitted light due to direct emission of the donor is minimal (5-10%). The strong FRET signal is evident from the large increase in the excitation intensity of the peaks between 300 and 350 nm. An especially useful feature of the pyrene/coumarin pair is that the presence of the donor affects neither the relative fluorescence nor the wavelength of the acceptor maximum. In each environment the intensity at 378 nm may be used as an internal standard for acceptor concentration and to confirm the absence of inner filter effects or other factors which may affect the measured fluorescence intensity.

Structural studies have shown that GpA forms a parallel homodimer in SDS, DDMAB, and DPC micelles (Bu & Engelman, 1999; Lemmon *et al.*, 1992b; MacKenzie *et al.*, 1997). To ensure that energy transfer was mediated by dimerization of GpA rather than the coincidence of two peptides present in the same micelle, the fluorescence was measured in the presence of unlabeled peptide. The spectra shown in Figure 6(a)-(c) focus on the FRET signal at 345 nm and the acceptor maximum at 378 nm. The intensity at 378 nm is useful for verfying that the acceptor concentration is constant within each experiment. The intensity at 345 nm, however, depends both on the addition of unlabeled GpA peptide and on the particular micelle environment. In each environment the intensity at 345 nm is reduced ~50% by the presence of unlabeled GpA peptide (equimolar with respect to total labeled peptides), whereas unlabeled control peptide has no effect. The independence of the FRET signal to the presence of unlabeled control peptide shows that there is indeed sufficient excess detergent to disperse the peptides. The ratio of the intensities at 345 nm and 378 nm ($I_{345\ nm}/I_{378\ nm}$) is much smaller in SDS (Figure 6(a)) than in DDMAB and DPC ((b) and

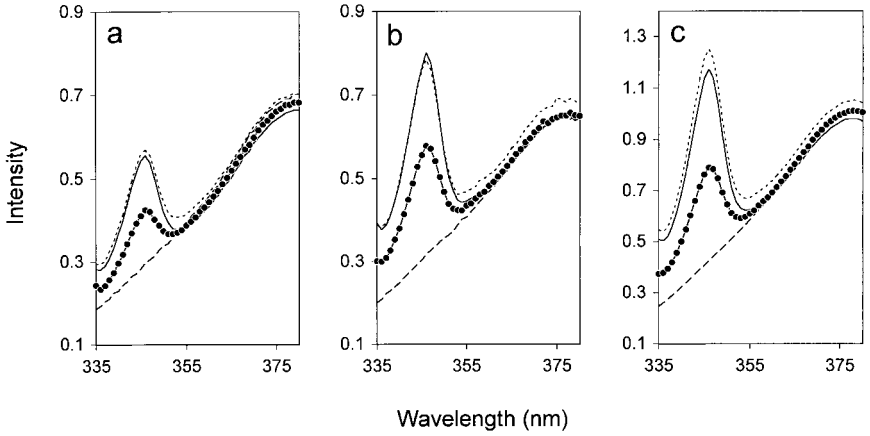

Figure 6. Competition by unlabeled GpA peptide in detergent micelles. Donor and acceptor peptides were mixed, equilibrated, and aliquoted into three fractions. After unlabeled GpA (· · ·), unlabeled control (- - -), or detergent (—) was added, the emission intensity was measured at 500 nm as a function of excitation wavelength and compared to a solution containing acceptor only (– – –). The final concentrations were 1.5 μM Pyr·GpA, 1.5 μM Cou·GpA, and 3.0 μM unlabeled peptide; (a) 9 mM SDS; (b) 25 mM DDMAB; (c) 25 mM DPC. The maximum theoretical ratio may be calculated using equation (5) as described in Material and Methods.

(c)). Comparison of the observed ratio $I_{345\ nm}/I_{378\ nm}$ to the maximum theoretical ratio calculated from the measured molar absorptivity indicates that the GpA dimer is less stable in SDS than in the two zwitterionic micelles. Reduction of the FRET signal by ~50 % specifically in the presence of GpA peptide, indicates that the FRET signal is proportional to the concentration of sequence-dependent heterodimers, and is thus a sensitive measure of the extent of association. Reduction by a value other than 50 % would have indicated problems, such as interference from the labels or lack of equilibration. Thus, regardless of the different oligomer stabilities competition with an unlabeled sample provides a relatively facile preliminary experiment to verify an oligomeric model, test for perturbation of the labels, and screen potentially important environmental variables.

Properties of the GpA oligomer revealed by FRET

The stoichiometry of donors and acceptors in the oligomer was determined to assess whether we had successfully reconstituted a dimer. The energy transfer was measured as a function of donor-acceptor ratio, while keeping the total peptide and detergent concentrations constant. In Figure 7 the total energy transfer (E) is plotted as a function of the mole fraction of acceptor ($X_{Acceptor}$). Energy transfer depends linearly on the acceptor mole fraction only when the oligomer is a dimer and the equilibrium constants of donor-donor, acceptor-acceptor, and donor-acceptor dimerization are the same (Stryer, 1978). For dimers, the energy transfer is described by equation (2):

$$E = E_i \times X_{Acceptor} \quad (2)$$

where E_i is the efficiency of energy transfer within a given heterodimer. The observed energy transfer extrapolates to a maximum value of 100 %, confirming our expectation that neither the distance between the donor and the acceptor nor their relative orientations would limit energy transfer. Thus, this donor-acceptor pair serve as a sensitive measure of dimer concentration without interference from possible changes in the details of the peptide structure in the monomer and dimer states.

The time required to reach equilibrium was determined by following the growth of the energy transfer signal until a steady state was achieved. As shown by the raw data presented in Figure 8(a), the intensity at the acceptor maximum (378 nm)

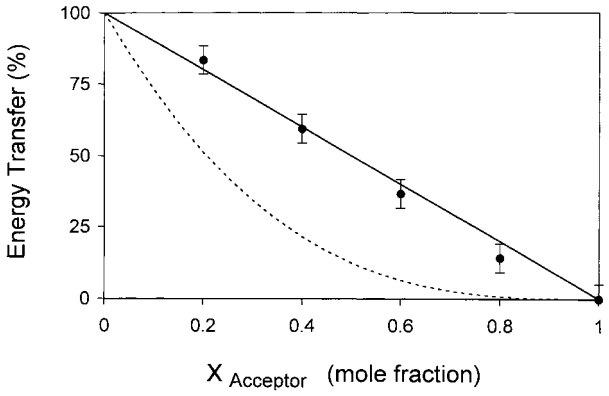

Figure 7. Stoichiometry of donors and acceptors. Energy transfer was calculated using equation (5) as described in Materials and Methods and is plotted as a function of the acceptor mole fraction. The ratio of Cou·GpA to Pyr·GpA was varied between 0.20 and 1.0 while keeping the total peptide concentration constant at 2.0 μM and the detergent concentration constant at 12.5 mM DDMAB. Calculated curves for dimer (—) and tetramer (- - -) when the equilibrium constants for donor-donor, donor-acceptor, and acceptor-acceptor association are the same.

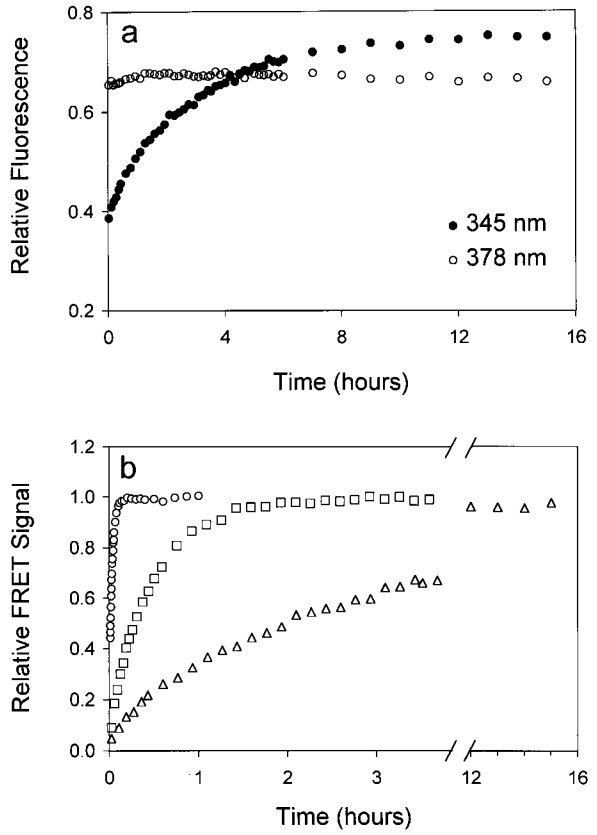

Figure 8. Kinetics of heterodimer formation. Growth of the energy transfer signal was monitored as a function of time in each detergent. Stock solutions of 4.0 μM Pyr·GpA and Cou·GpA were prepared, equilibrated, and mixed at a 1:1 molar ratio. The reaction was monitored over several hours by measuring the emission intensity at 500 nm as a function of excitation wavelength between 335 nm and 380 nm. (a) Equilibration in 25 mM DPC at 45 °C. Acceptor maximum at 378 nm (○), sensitized emission at 345 nm (●). (b) The ratio of intensity at 345 nm and 378 nm was normalized to the maximum ratio measured after 36 hours. Reaction conditions: 1.4 mM SDS at 25 °C (○), 25 mM DDMAB at 25 °C (□), 25 mM DPC at 45 °C (△). The temperature was elevated to 45 °C because the reaction in DPC did not equilibrate at 25 °C even after several days (data not shown). The temperature used by MacKenzie *et al.* for the NMR structure determination was 40 °C (MacKenzie *et al.*, 1997).

remained relatively constant throughout the reaction, while the intensity at 345 nm steadily increased from an initial value corresponding to the direct emission of the donor and acceptor. In order to facilitate comparison of the reaction in specific detergents without regard to changes in stability, the ratio of the intensity at 345 nm to 378 nm ($I_{345/348}$) was normalized to the maximum ratio observed after 36 hours. The time required to reach a steady state depended on the identity and concentration of the detergent and was in general at least tenfold shorter in SDS than in the zwitterionic detergents; SDS (~ten minutes), DDMAB (~two hours), and in DPC (>12 hours). These experiments indicate that modulation of the GpA dimerization kinetics by the micelle environment is indeed measurable using our FRET approach. Under these conditions, the reaction monitored by the FRET signal is an exchange reaction between homodimers to form heterodimers; DD + AA → 2 DA. Formation of heterodimers requires dissociation and reassociation of the peptides as well as diffusion and mixing of the micelles, therefore a detailed kinetic analysis must take into account the different number and properties of the micelles. At this preliminary stage we may conclude that the kinetics of GpA dimerization is modulated by features of the micellar environment even though we cannot distinguish specific properties important for micelle mixing from those important for peptide-peptide or peptide-micelle interactions. These experiments confirmed our expectation that this donor-acceptor pair provide a sensitive measure of the GpA monomer and dimer concentrations and allow us to study how specific features of the environment modulate the thermodynamics of transmembrane helix association.

It is worth noting however, that these data alone do not allow us to distinguish between dimer formation (DD + AA → 2 DA) and tetramer formation from the association of kinetically trapped dimers (DDDD + AAAA → 2 DDAA). In both reactions the change in oligomer order is by a factor of two. The latter reaction might occur if association of GpA dimers in a head-to-tail fashion is mediated by the opposite charges at the end of the transmembrane domain. Head-to-tail association is biologically irrelevant, but is a possible experimental artifact produced when the uniquely oriented membrane helices are extracted into an isotropic solvent (Challou *et al.*, 1994). In the SDS-PAGE experiment (see Figure 4), no tetramer band was detected and the exchange of homodimers to form heterodimers clearly depended on the GpA sequence known to form the helix-helix interface. Building on the independent structural measurements that have demonstrated the parallel geometry of the GpA dimer (Bu & Engelman, 1999; Lemmon *et al.*, 1992a; MacKenzie *et al.*, 1997), we used FRET to explore how specific features of the environment modulate the thermodynamics of transmembrane helix association.

Thermodynamics of the GpA dimer in SDS

The sensitivity of GpA dimerization to SDS concentration and temperature was investigated because of the unusual stability of the GpA dimer in SDS-PAGE, which is observed even after boiling. The dissociation constant was measured by serial dilution of the peptide while keeping the concentration of other components constant. In Figure 9(a) the fraction dimer is plotted as a function of the total peptide concentration in 5 mM SDS. The data measured at peptide concentrations ranging from 10 nM to 5 μM clearly correspond to

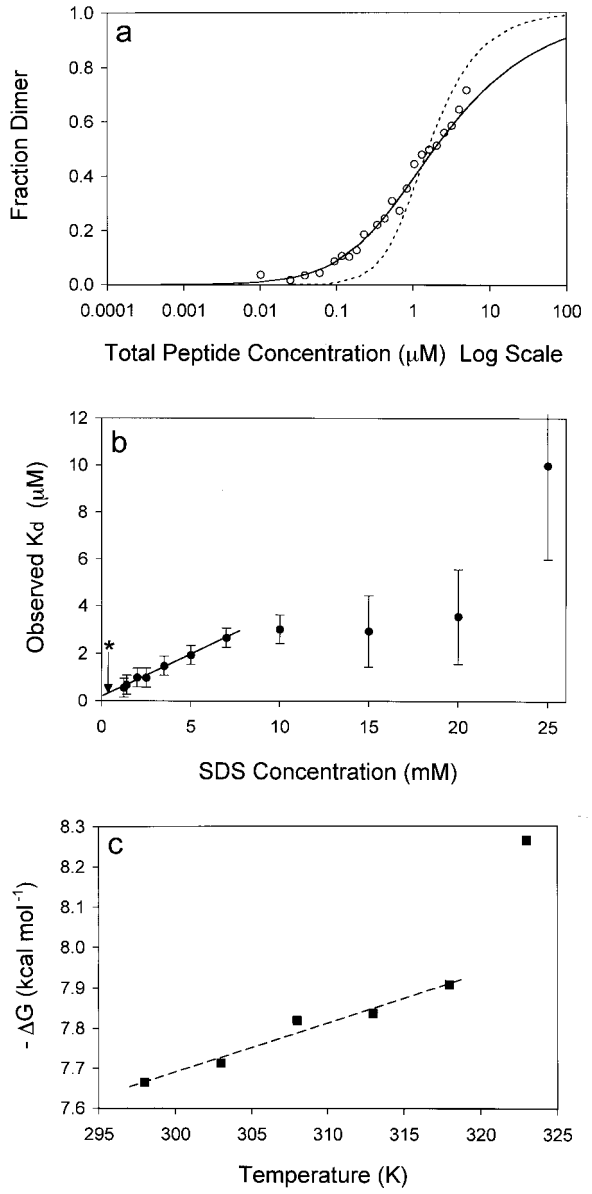

Figure 9. GpA dissociation in SDS micelles. Initial samples were prepared with an equimolar mixture of donor and acceptor labeled peptides at a total concentration of 5.0 μM. Total peptide concentration was varied by serial dilution, while the other components were held constant. Excitation spectra were collected and evaluated as described in Materials and Methods. The fraction dimer is plotted as a function of total peptide concentration; (a) 5 mM SDS at 25 °C. The continuous and broken lines are the expected curves for a dimer or a tetramer model, respectively. (b) The GpA dissociation constants were measured as a function of SDS concentration. The critical micelle concentration was measured as described in Materials and Methods; 65 μM in all our experimental conditions (★). (c) The reaction ΔG as a function of temperature was calculated from the K_d using 1 M as the standard state and considering SDS as a co-solute present at 7 mM.

the curve calculated for dimer dissociation according to equation (3) with a dissociation constant of 1.9(±0.4) μM:

$$K = \frac{[M]^2}{[D]} \quad (3)$$

The upper limit of the data (~5 μM) corresponds to the concentration at which the absorbance of the sample in a 3 mm cuvette is <0.05, the practical limit for avoiding inner filter effects. The lower detection limit is met when the background is >50 % of the total fluorescence, and thus depends both on environment and on temperature. The broken line describes the curve calculated for a tetramer-monomer dissociation, showing that we can indeed distinguish between a dimer and tetramer model even if the top of the curve can not be measured.

Since the detergent was expected to be the most important co-solute, we examined the effect of SDS concentration on the equilibrium using data derived from dissociation curves similar to the one shown in Figure 9(a) (listed in Table 1). In Figure 9(b) the observed K_d value is plotted as a function of the SDS concentration. For comparison the CMC measured in the absence of peptide (65 μM) is marked with an arrow. As the SDS concentration increases the measured dissociation constant also increases, from a dissociation constant of 0.56 μM in 1.2 mM SDS to a maximum observable value of ~10 μM in 25 mM SDS. The relationship shows two important features. First, the relationship between K_d and SDS concentration is linear up to ~7 mM though thereafter it may saturate. Second, the K_d at the critical micelle concentration of the detergent is non-zero. The possible saturation is consistent with SDS-PAGE experiments where significant dimer is still observed even in

Table 1. Observed GpA dissociation constants

Micelle environment	K_d (μM)	Excess detergent (mol:mol)
DDMAB[a]	0.08 ± 0.04	260,000
DPC[a]	0.16 ± 0.08	150,000
SDS (mM)		
25	~10	2200-3100
20	3.6	5600
15	2.9	5100
10	3.0	3300
7.0	2.7	2600
5.0	1.9	2500
3.5	1.5	2300
2.5	0.98	2500
2.0	0.99	2000
1.4	0.68	2000
1.2	0.56	2100

[a] Dissociation constants were measured in buffered solutions containing 25 mM detergent (or in SDS at the indicated concentration), at 25 °C, except in DPC at 45 °C. The micellar concentration was calculated from the total concentration by subtraction of the CMC (65 μM SDS; 4.3 mM DDMAB; 1 mM DPC, independent of temperature). The excess environment indicates the moles of micellar detergent per mole of peptide at the K_d.

the presence of very high detergent concentrations (69-100 mM). It should be borne in mind, however, that there are relatively large uncertainties associated with our K_d determinations at high detergent concentrations. The second point is also clear from the raw data where dilution of a sample with detergent-free buffer leads to a reduction in the degree of association (data not shown). Future work will investigate whether the dependence of the K_d on SDS indeed reaches a constant value.

The temperature dependence of the dissociation constant was measured in 7 mM SDS. The K_d is linear with temperature (Figure 9(c)) and can thus be evaluated with the van't Hoff equation. We were limited in the temperature range we could use; at the low end by SDS crystallization, and at the high end by fluorophore quenching. Therefore, for determination of the thermodynamic parameters, only the data in the linear region between 298 and 318 K were used. A rather small van't Hoff enthalpy of -3.6 kcal mol^{-1} is observed, corresponding to a specific enthalpy of only 0.9 cal g^{-1}. Under these conditions the observed change in the Gibb's free energy of the reaction depicted in Figure 1 is -7.6 kcal mol^{-1} at 25 °C and the entropic term contributes -3.9 kcal mol^{-1} (12 cal mol^{-1} K^{-1}). Recall that the observed K_d reflects the relative partitioning of detergent between binding to monomeric GpA, binding to dimeric GpA, and self-associating to form micelles. At this preliminary stage we may only conclude that there are temperature-dependent changes in any or all of the equilibria described by K_{GpA}, K_x, K_y, and K_{mic}, which on balance favor the GpA dimer as the temperature increases.

The observed dependence of the equilibrium on the aqueous solvent volume, on the concentration of SDS, and on temperature suggests that SDS should be considered as a co-solute rather than as a solvent. The solubility of GpA peptides in the absence of free SDS micelles indicates that the transfer of the SDS monomer from solution to the surface of the peptide is more favorable than SDS association to form micelles. Whenever this is true the CMC of the detergent measured in the absence of peptide provides an upper boundary on the free energy of GpA-detergent binding. Since in this case the free energy of GpA-SDS interaction is less than -5.7 kcal mol^{-1}, the contribution from the environment may provide a significant fraction of the total free energy of GpA-SDS complex. The measured enthalpic and entropic terms favoring GpA dimerization have the same order of magnitude as a single hydrogen bond. Based on these arguments, interactions between charged or polar side-chains and detergent head groups may be significant, even without specific binding. Extraction of the protein-protein ΔG, ΔH, and ΔS requires a better understanding of the interactions between the protein and the detergent, which we hope will be possible to acquire using techniques we describe here. Direct interpretation of observed K_d as ΔG, may be possible when conditions are defined where changes in relative solubility of the monomer and dimer peptides perturb the association free energy by less than $\approx$0.5 kcal mol^{-1}, the current precision of available measurements. These experiments demonstrate that our approach will allow detailed thermodynamic exploration of the role of sequence and the environment revealed by the structural and mutagenesis data describing the GpA transmembrane helix dimer.

Thermodynamics of the GpA dimer in zwitterionic detergents

Relative to the strong denaturant SDS, it was expected that the GpA dimer would be more stable in zwitterionic detergents considered to provide a more ''native-like'' membrane mimetic environment. The preliminary measurements in two zwitterionic detergents are shown in Figure 10; in 25 mM DDMAB at 25 °C (a) and in 25 mM DPC at 45 °C (b). The elevated temperature used in DPC experiments was necessary to obtain a reasonable rate of equilibration. Although the detection

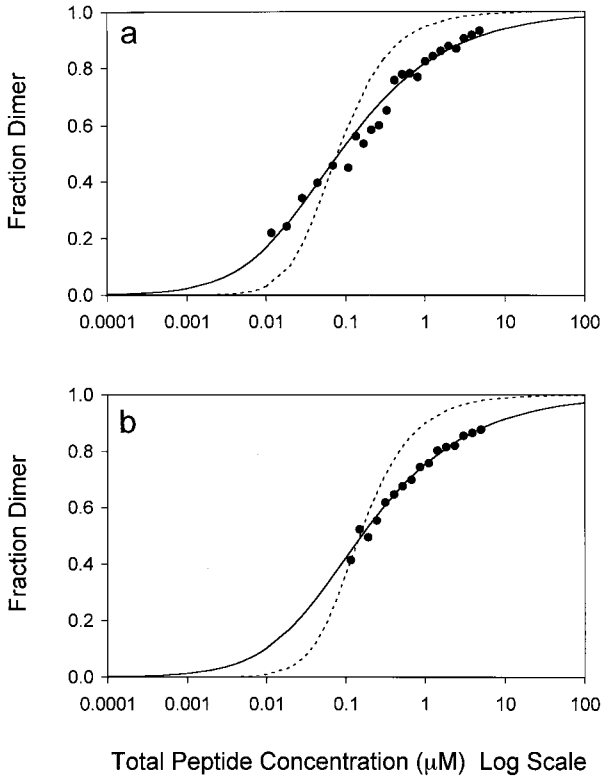

Figure 10. GpA dissociation in zwitterionic micelles. Initial samples were prepared with an equimolar mixture of donor and acceptor labeled peptides at a total concentration of 5.0 μM. Total peptide concentration was varied by serial dilution, while the other components were held constant. Excitation spectra were collected and evaluated as described in Materials and Methods. The fraction dimer is plotted as a function of total peptide concentration. The continuous and dotted lines are the expected curves for a dimer or a tetramer model, respectively; (a) 25 mM DDMAB at 25 °C; (b) 25 mM DPC at 45 °C.

limits of the data vary (see above and Materials and Methods), the data correspond to dissociation constants 0.08(±0.4) μM in DDMAB and 0.16(±0.8) μM in DPC. The dotted line describes the curve calculated for a tetramer-monomer dissociation, showing that we can indeed distinguish between a dimer and tetramer model even the measurable range is limited by background fluorescence or temperature quenching. Future experiments will explore the effect of detergent concentration and temperature on the K_d. Nevertheless, these preliminary measurements show that dissociation of the GpA dimer is measurable even if it is several orders of magnitude more stable than it is in SDS.

As a first estimate of the coupling between the peptide and environment we compared the molar excess of the detergent in the micellar phase at the midpoint of the GpA dissociation reaction. The amount of detergent in the micelle phase was estimated by subtracting the CMC from the total concentration: 65 μM SDS, 4.3 mM DDMAB, and 1 mM DPC (see Materials and Methods). As can be seen from the data in Table 1, the amount of surfactant required to achieve 50 % dissociation of the GpA dimer is two orders of magnitude higher in the zwitterionic micelles than it is in SDS. The trend in the GpA K_d with micellar SDS does not yield a constant peptide:SDS ratio, suggesting that the GpA-SDS environmental term is also dependent on the SDS concentration. Although at this preliminary stage these equilibrium constants cannot be interpreted directly as GpA dissociation free energies, the data demonstrate the stability of the GpA dimer, since it remains associated even in the presence of a vast excess of micelles.

The relative stability of the GpA dimer in DDMAB and DPC is consistent with the retained function of membrane proteins in zwitterionic environments (Brenner *et al*., 1995; Kessi *et al*., 1994), which depends in part on the maintenance of transmembrane helix association. In addition, the relative destabilization of the GpA dimer in SDS, ~2 kcal mol^{-1}, is of roughly the same magnitude as mutations that disrupt packing at the dimer interface (1-3 kcal mol^{-1}) as estimated in SDS-PAGE (Lemmon *et al*., 1992b; Mingarro *et al*., 1997), deduced from the NMR structure (MacKenzie & Engelman, 1998), and measured by small-angle X-ray scattering (Bu & Engelman, 1999), or by analytical ultracentrifugation (Fleming *et al*., 1997). Together with measurements of secondary structure and detergent binding, the approach we describe will allow the thermodynamic factors favoring and opposing GpA dimerization to be explored in specific chemical terms.

Conclusions

Our approach to use labeled peptides and to measure oligomerization through sensitized emission combines several advantages for quantitative measurements. First, the synthetic approach allows unique and complete labeling of the polypeptides. Second, the composition of the membrane-mimetic environment is not complicated by co-purification of components from *E. coli*. Third, sensitized emission may be used to detect FRET even when interactions with the environment may affect the donor quantum yield differently in the monomeric and oligomeric states. Fourth, because the sensitized emission from the donor pyrene is localized to 300-350 nm, the acceptor maximum near 380 nm may be used as an internal control for acceptor concentration. We have shown that the labels neither interfere with detection of secondary structure nor with migration and association in SDS-PAGE, and that the labels are useful for measuring equilibrium constants over several orders of magnitude. The approach is limited by current synthetic efficiencies to domains <60 amino acid residues, by potential interference from UV absorbing contaminants, by inner-filter effects, and by quenching at high temperature. Despite these caveats, the approach is applicable in a wide range of environments and we expect it will be useful for exploring the relative importance of environmental factors in the kinetics and thermodynamics of integral membrane protein assembly.

In contrast to soluble coiled-coils in which helix formation is coupled to oligomerization, we have shown that GpA helix formation is independent of dimerization. The secondary structure of the GpA monomer and dimer in SDS are the same as the secondary structure of the GpA dimer in the zwitterionic detergents, DDMAB and DPC (in which the structure was solved). This finding implies that we are justified in comparing thermodynamic measurements in these environments, since we are measuring helix association uncomplicated by changes in the stability of the helix or by changes in the structure of other domains. The insensitivity of the secondary structure to the details of the micelle environment support the thermodynamic rationale for stage I of the model described by Popot & Engelman (1990), that independent helices are stable because of the strength of hydrogen bonds in a low dielectric environment. These CD measurements of the GpA monomer peptide in SDS have confirmed a long-standing assumption that glycophorin A is an integral membrane protein for which formation of the monomer helix is both energetically and physically distinct from formation of the dimer. These data provide additional support for the view that dimerization of the GpA transmembrane domain in SDS-PAGE is stabilized by van der Waals interactions between complementary surfaces of independently stable helices.

Our findings that the GpA dimer is about two orders of magnitude less stable in SDS than it is in zwitterionic environments and the strong effect of environment concentration both suggest that the environment may have as large an impact on helix association as do mutations at helix-helix interfaces. The free energy of GpA helix dimeriza-

tion results from favorable enthalpic and entropic terms, each contributing -4 kcal mol^{-1} to ΔG in 7 mM SDS. It appears likely that the burial of $\approx$400 Å^2 and the concomitant release of SDS provides at least half of the free energy favoring dimerization. These measurements provide a foundation for understanding the stability of the GpA dimer in SDS and emphasize the role of the lipidic environment in the folding of membrane proteins.

Materials and Methods

Preparation of labeled peptides

Peptides corresponding to residues 69-101 of human glycophorin A were synthesized with an Applied Biosystems model 430 peptide synthesizer (Applied Biosystems, Inc., Foster City, CA) using an Fmoc strategy and PEG-PS resin. Labeling with pyrene acetic acid or with 7-dimethylaminocoumarin-4-acetic acid (Molecular Probes, Eugene, OR) was accomplished through peptide bond formation as described (Wendt *et al*., 1995). Free amino and carboxyl termini were blocked with acetyl or amide, respectively. Peptides were purified by three rounds of reversed-phase high performance liquid chromatography on a semi-preparative Zorbax cyano-propyl column with a water/acetonitrile gradient containing 0.3 % (v/v) trifluoroacetic acid. After purification to greater than 99 % purity as determined by integrated peak intensities, mass spectrometry was used to confirm the presence of a single peptide corresponding to the predicted molecular mass. Amino acid analysis was used to further confirm the purity and identity of the peptides. Amino acid correlation coefficients for the samples used in this study were $R \geqslant 0.99$ (data not shown).

Purification and characterization of detergents

DDMAB was purchased from Calbiochem, and was re-crystallized twice from methanol/acetone to remove most of the UV-absorbing contaminants (Chevalier *et al*., 1991). Ultrapure electrophoresis grade sodium dodecyl sulfate was purchased from Gibco BRL (Grand Island, NY). The same lot of SDS was used for all the experiments because the association of membrane proteins in SDS-PAGE is known to be affected by variation in lot composition. Dodecyl phosphocholine (DPC) (purity >99 %) (Avanti Polar Lipids, Alabaster, AL) was used without further purification. The critical micelle concentrations (CMC) were measured as the point at which the relative surface tension became independent of the concentration of the surfactant, or by ANS fluorescence (De Vendittis *et al*., 1981). The CMC values were independent of temperature and were consistent with reported values (Chevalier *et al*., 1996; Kamenka *et al*., 1995; Lauterwein *et al*., 1979); 65 μM SDS, 4.3 mM DDMAB, and 1 mM DPC.

Reconstitution into micelles

The HPLC fractions containing peptide were concentrated and exchanged into doubly distilled trifluoroethanol by rotary evaporation to achieve a peptide concentration of 10-20 μM. Two methods were employed to reconstitute the peptide into micelles. The samples were diluted with buffered detergent, lyophilized, and dissolved with water. Alternatively, the samples were diluted with water (50 %, v/v), lyophilized, and dissolved with buffered detergent. Final concentrations were 9-120 μM peptide, 5-67 mM detergent, 200 mM sodium chloride buffered at 25 °C with 20 mM sodium phosphate to pH 7.0. A potassium hydroxide pellet trap was included during lyophilization to help remove residual trifluoroacetic acid, which can be detected by a peak at 1685 cm^{-1} by Fourier transform infrared spectroscopy. If necessary, residual trifluoroacetic acid was removed by dialysis. The UV, CD, and fluorescence spectra obtained from samples reconstituted by either method were indistinguishable. The concentration of the detergent will be indicated for each experiment.

SDS-PAGE competition assay

The assay was similar to that described by Lemmon *et al*. (1992a). Samples were mixed with an equal volume of Laemmli buffer, heated at 80 °C for two minutes, assayed on a PhastSystem 20 % polyacrylamide gel (Pharmacia, Uppsala, Sweden) and stained with Coomassie brilliant blue.

Spectroscopy

Absorption spectra were recorded either on a Perkin Elmer Lambda 6 (Perkin Elmer, Norwalk, CT) or on a Cary 5 (Varian, Sydney, Australia) spectrophotometer using either a 3 mm or a 1 cm pathlength cuvette. Peptide concentrations ranged from 12 to 25 μM while detergent concentrations ranged from 5 mM to 67 mM. Extinction coefficient spectra were calculated using the concentrations determined by amino acid analysis. The uncertainties noted are two times the estimated standard deviation of at least four independently reconstituted samples and are larger than the propagated uncertainties calculated using the Student t test for the 95 % confidence limit, (Schoemaker *et al*., 1989). The extinction coefficients determined in trifluoroethanol varied by as much as 50 %, presumably due to variations in the amount of residual trifluoroacetic acid in each purified preparation. After reconstitution removal of residual trifluoroacetic acid was confirmed by the absence of a band at 1685 cm^{-1} in Fourier transform infrared spectroscopy.

Far UV circular dichroism spectra (CD) were recorded on an Aviv 62DS spectrophotometer (Lakewood, NJ) using either a 0.1 mm or a 0.1 cm pathlength cuvette at peptide concentrations ranging from 9-120 μM. Typically spectra were acquired with a resolution of 0.5 nm, a four seconds integration time, and four scans were averaged prior to background subtraction. The dynode voltage was recorded, and several concentrations were measured to ensure that neither absorption flattening nor differential light scattering reduced the apparent ellipticity. To simplify the comparison between different samples and to verify the average secondary structure content, ellipticity spectra were converted from millidegrees to mean residue ellipticity, according to equation (4):

$$\text{Mean residue ellipticity} = \frac{100\ \theta}{cnl} \qquad (4)$$

where θ is the measured ellipticity in mdeg, c the peptide concentration in μM, n the number of amino acids in the peptide, and l the pathlength in cm. Except for the peptide concentration, the solution conditions matched those in the fluorescence measurements.

Steady-state fluorescence spectra were recorded on either an SLM 8000 (SLM, Spectronics Instruments, Rochester, NY) or a SPEX fluorolog (SPEX, Longjumea, France) in each case equipped with a R928 Hammamatsu photomultiplier. Typically spectral resolution of the excitation and emission monochromators were set at 2 nm and 10 nm, respectively. Excitation spectra between 250 and 450 nm were recorded measuring the emission at 500 nm relative to the reference channel, which corrects for the wavelength dependence of the excitation intensity. Samples were measured in a stoppered 3 mm cuvette with and without degassing. Although oxygen reduced the donor and acceptor intensity it did not affect the ratio of the intensity used for FRET. The upper limit of the data (~5 μM) corresponds to the concentration at which the absorbance of the sample in a 3 mm cuvette is <0.05, the practical limit for avoiding inner filter effects. The lower detection limit is met when the background is >50% of the total fluorescence, and thus depends both on the spectral properties of the environment and on temperature.

For calculations of fluorescence yield, emission spectra were collected at a spectral resolution of 2 nm and corrected for the response function of the detection system. Quantum yields were calculated by comparison of the integrated intensity of the emission spectrum with that of quinine sulfate in 1 N H_2SO_4 adjusted to give an identical absorption at the excitation wavelength. The quantum yield of quinine sulfate was taken to be 0.55 (Chen, 1967; Melhuish, 1964). Energy transfer was detected by sensitized emission, and calculated according to equation (5) (Stryer, 1978):

$$E = \left[\frac{G(\lambda_2)}{G(\lambda_1)} - \frac{\varepsilon_A(\lambda_2)}{\varepsilon_A(\lambda_1)}\right] \times \frac{\varepsilon_A(\lambda_1)}{\varepsilon_D(\lambda_2)} \qquad (5)$$

The acceptor excitation spectra (G) and the extinction coefficients (ε) were used to choose λ_1, where the donor has minimal absorption, and λ_2, where the extinction coefficient of the donor is large relative to the extinction coefficient of the acceptor.

Acknowledgments

We thank N. Zondlo and M. Cocco for technical suggestions that resulted in significant improvements in synthetic and purification yields, M. Crawford (Boyer Center for Molecular Medicine) for amino acid analysis, Professor J. Doudna for the use of the mass spectrometer, K. Mitra and W. McMurray (Yale Comprehensive Cancer Center) for mass spectrometry measurements, and Z. Bu for many helpful discussions. We thank M. Bowen, M. Cocco, A. Lee, K. MacKenzie, K. Mitra, B. Russ, A. Senes, K. Sonoda, I. Uberratxena, and F. Zhou for critical reading of the manuscript. D.M.E. thanks the region Ile de France and the Ecole Normale Supérieure, Paris, for their sponsorship of the Blaise Pascal Chair. This work was supported by grants from the NSF and NIH, NSF-MCB-9406983 and NIH-GM-54160.

References

Adair, B. D. & Engelman, D. M. (1994). Glycophorin A helical transmembrane domains dimerize in phospholipid bilayers: a resonance energy transfer study. *Biochemistry,* **33**, 5539-5544.

Adams, P. D., Engelman, D. M. & Brünger, A. T. (1996). Improved prediction for the structure of the dimeric transmembrane domain of glycophorin A obtained through global searching. *Proteins: Struct. Funct. Genet.* **26**, 257-261.

Booth, P. J., Riley, M. L., Flitsch, S. L., Templer, R. H., Farooq, A. & Curran, A. R. (1997). Evidence that bilayer bending rigidity affects membrane protein folding. *Biochemistry,* **36**, 197-203.

Boyd, D., Schierle, C. & Beckwith, J. (1998). How many membrane proteins are there? *Protein Sci.* **7**, 201-205.

Brenner, C., Jan, G., Chevalier, Y. & Wroblewski, H. (1995). Evaluation of the efficacy of zwitterionic dodecyl carboxybetaine surfactants for the extraction and the separation of mycoplasma membrane protein antigens. *Anal. Biochem.* **224**, 515-523.

Bu, Z. & Engelman, D. M. (1999). A method for determining transmembrane helix association and orientation in detergent micelles using small angle X-ray scattering. *Biophys. J.* **77**, 1064-1073.

Challou, N., Goormaghtigh, E., Cabiaux, V., Conrath, K. & Ruysschaert, J. (1994). Sequence and structure of the membrane-associated peptide of glycophorin A. *Biochemistry,* **33**, 6902-6910.

Chen, R. F. (1967). Some characteristics of the fluorescence of quinine. *Anal. Biochem.* **19**, 374-387.

Chevalier, Y., Storet, Y., Pourchet, S. & Perchec, P. L. (1991). Tensioactive properties of zwitterionic carboxybetaine amphiphiles. *Langmuir,* **7**, 848-853.

Chevalier, Y., Kamenka, N., Chorro, M. & Zana, R. (1996). Aqueous solutions of zwitterionic surfactants with varying carbon number of the intercharge group. 3. Intermicellar interactions. *Langmuir,* **12**, 3225-3232.

De Vendittis, E., Palumbo, G., Parlato, G. & Bocchini, V. (1981). A fluorimetric method for the estimation of the critical micelle concentration of surfactants. *Anal. Biochem.* **115**, 278-286.

Fleming, K. G., Ackerman, A. L. & Engelman, D. M. (1997). The effect of point mutations on the free energy of transmembrane α-helix dimerization. *J. Mol. Biol.* **272**, 266-275.

Haltia, T. & Friere, E. (1995). Forces and factors that contribute to the structural stability of membrane proteins. *Biochim. Biophys. Acta,* **1241**, 295-322.

Haugland, R. P. (1996). *Handbook of Fluorescent Probes and Research Chemicals* (Spence, M. T. Z., ed.), Molecular Probes, Inc., Eugene, OR.

Huang, K. S., Bayley, H., Liao, M. J., London, E. & Khorana, H. G. (1981). Refolding of an integral membrane protein. *J. Biol. Chem.* **256**, 3802-3809.

Kamenka, N., Chevalier, Y. & Zana, R. (1995). Aqueous solutions of zwitterionic surfactants with varying carbon number of the intercharge group. 1. Micelle aggregation numbers. *Langmuir,* **11**, 3351-3355.

Kessi, J., Poiree, J. C., Wehrli, E., Bachofen, R., Semenza, G. & Hauser, H. (1994). Short-chain phosphatidylcholines as superior detergents in solubilizing membrane proteins and preserving biological activity. *Biochemistry,* **33**, 10825-10836.

Killian, J. A. (1998). Hydrophobic mismatch between proteins and lipids in membranes. *Biochim. Biophys. Acta,* **1376**, 401-416.

Langosch, D., Brosig, B., Kolmar, H. & Fritz, H. J. (1996). Dimerization of the glycophorin A transmembrane segment in membranes probed with the ToxR transcription activator. *J. Mol. Biol.* **263**, 525-530.

Lau, F. W. & Bowie, J. U. (1997). A method for assessing the stability of a membrane protein. *Biochemistry,* **36**, 5884-5892.

Lauterwein, J., Bosch, C., Brown, L. R. & Wüthrich, K. (1979). Physicochemical studies of the protein-lipid interactions in melittin-containing micelles. *Biochim. Biophys. Acta,* **556**, 244-264.

Lee, A. G. (1998). How lipids interact with an intrinsic membrane protein: the case of the calcium pump. *Biochim. Biophys. Acta,* **1376**, 381-390.

Leeds, J. A. & Beckwith, J. (1998). Lambda repressor N-terminal DNA-binding domain as an assay for protein transmembrane segment interactions *in vivo*. *J. Mol. Biol.* **280**, 799-810.

Lemmon, M. A., Flanagan, J. M., Hunt, J. F., Adair, B. D., Bormann, B. J. & Dempsey, C. E. (1992a). Glycophorin A dimerization is driven by specific interactions between transmembrane α-helices. *J. Biol. Chem.* **267**, 7683-7689.

Lemmon, M. A., Flanagan, J. M., Treutlein, H. R., Zhang, J. & Engelman, D. M. (1992b). Sequence specificity in the dimerization of transmembrane alpha-helices. *Biochemistry,* **31**, 12719-12725.

MacKenzie, K. R. (1997). Structure determination of the dimeric membrane spanning domain of glycophorin A in detergent micelles by triple resonance nuclear magnetic resonance spectroscopy. PhD thesis, Yale University, New Haven, CT.

MacKenzie, K. R. & Engelman, D. M. (1998). Structure-based prediction of the stability of transmembrane helix-helix interactions: the sequence dependence of glycophorin A dimerization. *Proc. Natl Acad. Sci. USA,* **95**, 3583-3590.

MacKenzie, K. R., Prestegard, J. H. & Engelman, D. M. (1997). A transmembrane helix dimer: structure and implications. *Science,* **276**, 131-133.

Melhuish, W. H. (1964). Measurement of quantum efficiencies of fluorescence and phosphorescence and some suggested luminescence standards. *J. Opt. Soc. Am.* **54**, 183-186.

Mingarro, I., Elofsson, A. & von Heijne, G. (1997). Helix-helix packing in a membrane-like environment. *J. Mol. Biol.* **272**, 633-641.

Mouritsen, O. G. & Bloom, M. (1993). Models of lipid-protein interactions in membranes. *Annu. Rev. Biophys. Biomol. Struct.* **22**, 145-171.

Patel, L. R., Curran, T. & Kerppola, T. K. (1994). Energy transfer analysis of fos-jun dimerization and DNA binding. *Proc. Natl Acad. Sci. USA,* **91**, 7360-7364.

Popot, J. & de Vitry, C. (1990). On the microassembly of integral membrane proteins. *Annu. Rev. Biophys. Biophys. Chem.* **19**, 369-403.

Popot, J. & Engelman, D. M. (1990). Membrane protein folding and oligomerization: the two-stage model. *Biochemistry*, **29**, 4031-4037.

Russ, W. P. & Engelman, D. M. (1999). TOXCAT: A measure of transmembrane helix association in a biological membrane. *Proc. Natl Acad. Sci. USA,* **96**, 863-868.

Sami, M. & Dempsey, C. (1988). Hydrogen exchange from the transbilayer hydrophobic peptide of glycophorin reconstituted in lipid bilayers. *FEBS Letters,* **240**, 211-215.

Schoemaker, D. P., Garland, C. W. & Nibler, J. W. (1989). *Experiments in Physical Chemistry*, 5th edit., McGraw-Hill, New York.

Schulte, T. H. & Marchesi, V. T. (1979). Conformation of human erythrocyte glycophorin A and its constituent peptides. *Biochemistry,* **18**, 275-280.

Smith, S. O., Jonas, R., Braiman, M. & Bormann, B. J. (1994). Structure and orientation of the transmembrane domain of glycophorin A in lipid bilayers. *Biochemistry,* **33**, 6334-6341.

Stowell, M. H. B. & Rees, D. C. (1995). Structure and stability of membrane proteins. *Advan. Protein Chem.* **46**, 279-311.

Stryer, L. (1978). Fluorescence energy transfer as a spectroscopic ruler. *Annu. Rev. Biochem.* **47**, 819-846.

Sturgis, J. N. & Robert, B. (1994). Thermodynamics of membrane polypeptide oligomerization in light-harvesting complexes and associating structural changes. *J. Mol. Biol.* **238**, 445-454.

Treutlein, H. R., Lemmon, M. A., Engelman, D. M. & Brunger, A. T. (1992). The glycophorin A transmembrane domain dimer: sequence-specific propensity. *Biochemistry,* **31**, 12726-12732.

van der Meer, B. W., Coker, G. I. & Chen, S.-Y. S. (1994). *Resonance Energy Transfer: Theory and Data*, VCH Publishers, Inc., New York.

van Klompenburg, W., Nilsson, I., von Heijne, G. & de Kruijff, B. (1997). Anionic phospholipids are determinants of membrane topology. *EMBO J.* **16**, 4261-4266.

Veatch, W. & Stryer, L. (1977). The dimeric nature of the gramicidin A transmembrane channel: conductance and fluorescence energy transfer studies of hybrid channels. *J. Mol. Biol.* **113**, 89-102.

Wallin, E. & von Heijne, G. (1998). Genome-wide analysis of integral membrane proteins from eubacterial, archean, and eukaryotic organisms. *Protein Sci.* **7**, 1029-1038.

Wendt, H., Berger, C., Baici, A., Thomas, R. M. & Bosshard, H. R. (1995). Kinetics of folding of leucine zipper domains. *Biochemistry,* **34**, 4097-4107.

White, S. H. & Wimley, W. C. (1998). Hydrophobic interactions of peptides with membrane interfaces. *Biochim. Biophys. Acta,* **1376**, 339-352.

Zhou, N. E., Zhu, B.-Y., Kay, C. M. & Hodges, R. S. (1992). The two-stranded α-helical coiled-coil is an ideal model for studying protein stability and subunit interactions. *Biopolymers,* **32**, 419-426.

Edited by G. von Heijne

(Received 12 April 1999; received in revised form 6 August 1999; accepted 18 August 1999)